Engineering Science and Technology, an International Journal xxx (2018) xxx–xxx

HOSTED BY

ELSEVIER

Contents lists available at ScienceDirect

Engineering Science and Technology, an International Journal

journal homepage: www.elsevier.com/locate/jestch

Full Length Article

Electrical Impedance Spectroscopy (EIS) characterization of saline solutions with a low-cost portable measurement system

Marco Grossi [a,*], Carola Parolin [b], Beatrice Vitali [b], Bruno Riccò [a]

[a] Department of Electrical Energy and Information Engineering "Guglielmo Marconi" (DEI), University of Bologna, Bologna, Italy
[b] Department of Pharmacy and Biotechnology (FaBiT), University of Bologna, Bologna, Italy

ARTICLE INFO

Article history:
Received 7 May 2018
Revised 24 July 2018
Accepted 27 August 2018
Available online xxxx

Keywords:
Impedance Spectroscopy
Measurement
Frequency
Sensor
Portable system

ABSTRACT

Electrical Impedance Spectroscopy (EIS), a powerful technique used for wide range of applications, is usually carried out by means of benchtop instrumentation (LCR meters and ìmpedance analyzers), not suited for in-the-field measurements performed outside a laboratory.

In this paper a new portable electronic system for EIS on liquid and semi-liquid media is presented that is capable to produce an electrical fingerprint of the sample under investigation. The proposed system was used for the characterization of four different saline solutions (NaCl, Na_2CO_3, K_2HPO_4 and $CuSO_4$). A multi-frequency approach, based on the measurement of maximum value of the impedance imaginary component and its corresponding frequency, was tested for the first time to discriminate different saline solutions. The results show that the proposed method is capable to discriminate the different solutions and to measure the concentration ($R^2 = 0.9965$) independently of the type of saline solution.

1. Introduction

Electrical Impedance Spectroscopy (EIS) is a technique used in a wide range of applications [1]: from detection of bacterial concentration [2–8] to the analysis of human body composition [9–12], the characterization and quality assessment of different foods [13–18] as well as the investigation of corrosion of metals [19–21] and coated metal surfaces [22–24]. Other applications of EIS include the characterization of state-of-charge and state-of-health of batteries and fuel cells [25–28], the automated titration for different compounds [29] and the detection of cancer cells [30–34].

EIS was used for the first time in 1894 by W. Nerst to measure the dielectric constant of different types of electrolytes [35]. However, it was only in the 1980s that the use of this technique really ramped up, thanks to computer-controlled laboratory instrumentation that allowed much easier implementations. A conference dedicated to research and applications of EIS is held every three years and the number of publications on the subject doubles every four or five years, with about 1200 papers published in 2006 [36].

Today EIS investigations are usually carried out using dedicated benchtop instruments, such as LCR meters and Impedance Analyzers, that provide: a) accurate measurements on a wide range of frequencies; b) a variety of operative modes (i.e. 2, 3 or 4 electrodes measurements); c) interfaces toward computers to transfer the acquired data for filing and further processing. Moreover, many commercial instruments are sold with proprietary software for EIS data analysis, where the acquired data are fitted by means of a user-selectable equivalent circuit made of resistors, capacitors and inductors, as well as of non-linear empirical elements such as Constant Phase Elements (CPE) [37] and Warburg impedances [38]. However such scientific instruments are not suitable for in-situ and on-line analysis outside a laboratory.

On the other hand there are many applications requiring measurements outside a laboratory, such as for example: detection of milk adulteration [39] and clinical mastitis in cow's milk [40]; the analysis and characterization of fruits [41]; monitoring of alcoholic fermentation in wine [42]; detection of artificial chemical additives in liquid food products [43]; measurements of phenolic compounds' concentration in water [44]; analysis of petroleum products and characterization of water-in-oil emulsions [45]; detection of the underpaint corrosion of metallic surfaces [46].

Thus, in recent years, much effort has been devoted to the development of portable impedance analyzers to be used for in-situ EIS applications. This has become even simpler with the introduction on the market of the IC AD5933 (Analog Devices) [47], a low-cost on-chip impedance analyzer that can perform measurements in the impedance range 1 kΩ–10 MΩ (that can be extended to 100 Ω–10 MΩ with additional hardware) and frequency range

* Corresponding author.
E-mail address: marco.grossi8@unibo.it (M. Grossi).
Peer review under responsibility of Karabuk University.

https://doi.org/10.1016/j.jestch.2018.08.012
2215-0986/

1 kHz–100 kHz. Portable [48–50], wearable [51] as well as Smartphone based [52,53] impedance analyzers based on AD5933 have been proposed in literature.

In this paper a new low-cost (about 100 USD) portable instrument for EIS analysis of liquid and semi-liquid media is presented. Such a system, built using a 3D printer, features a microcontroller based board for measurements and data transfer to a laptop PC. Differently from other portable instruments for EIS measurements discussed in literature, the proposed instruments does not feature the IC AD5933 but uses an external waveform generator IC (AD5932) to generate the test signal and acquires the resulting signals using the analog-to-digital converters embedded in the microcontroller. This results in a reduction of the overall cost for the system as well as in the possibility to select different values for the amplitude of the AC test signal. Since it can be used by anyone and everywhere, it is suitable for in-field measurements outside a laboratory.

The proposed system has been tested to measure the concentration of different saline solutions, important particularly (but not exclusively) in the environmental monitoring, in the medical and biological fields since they are widely used as a vehicle to inject pharmaceuticals or as a supporting medium for biological and microbiological applications [54]. The obtained experimental results have shown that our system is able to estimate the solution concentration with good accuracy ($R^2 > 0.99$) independently of the type of saline solution.

2. Experimental approach

The proposed system ($10 \times 12 \times 18$ cm), shown in Fig. 1, is composed of a Polylactic Acid (PLA) structure realized with a 3D printer (MakerBot Replicator Z18) and an ad-hoc designed electronic board devoted to EIS measurements on samples hosted in disposable polypropylene containers. The system features a couple of cylinder shaped (radius 2.25 mm, length 5 mm, spaced 22 mm) stainless steel electrodes in direct contact with the Sample Under Test (SUT), hosted inside a 40 ml container. A temperature sensor (B57045K produced by TDK) is integrated on the electronic board to measure the SUT temperature, assumed to be in thermal equilibrium with the environment.

2.1. EIS basics

The proposed system performs EIS measurements in potentiostatic mode. Thus, a sine-wave voltage test signal

$$V_{in}(t) = V_{M,in} \cdot \sin(\omega t) \tag{1}$$

is applied between the two electrodes and the current through them

$$I_{in}(t) = I_{M,in} \cdot \sin(\omega t + \varphi) \tag{2}$$

is measured. In the above equations, $V_{M,in}$ and $I_{M,in}$ are the voltage and current amplitude, respectively; $\omega = 2\pi f$ is the angular frequency (with f the frequency of the test signal); φ is the phase difference between $I_{in}(t)$ and $V_{in}(t)$. From equations (1) and (2) the complex impedance Z can be calculated as:

$$Z(j\omega) = \frac{V_{in}(j\omega)}{I_{in}(j\omega)} = \frac{V_{M,in}}{I_{M,in}} \cdot e^{-j\varphi} = Re(Z) + j \cdot Im(Z) \tag{3}$$

where $V_{in}(j\omega)$ and $I_{in}(j\omega)$ are the Steinmetz transforms of $V_{in}(t)$ and $I_{in}(t)$.

A sequence of test signals with increasing frequencies is applied to the SUT and the impedance, as well as its real and imaginary components Re(Z) and Im(Z), are calculated for all applied frequencies.

The acquired spectrum is normally displayed using either the Bode plots, where Re(Z) and Im(Z), or alternatively the corresponding admittance components Re(Y) and Im(Y), are plotted vs. frequency (in logarithmic scale), or the Nyquist plot, where the Im (Z) or Im(Y) is plotted vs. the corresponding Re(Z) or Re(Y) for all the investigated frequencies.

Usually, the measured data are fitted with an equivalent electrical circuit and the circuit parameters are used to investigate the correlation with the SUT parameters of interest. In our case, the data fitting procedure is made by means of the software tool Multiple Electrochemical Impedance Spectra Parameterization (MEISP) v 3.0 by Kumho Chemical Laboratories.

2.2. Electronic board for EIS measurement

The electronic board of our system, designed ad-hoc using the software Kicad [55], is interfaced with a Nucleo STM32 development board (STM32F303 microcontroller by ST Microelectronics), that features a built-in UART-to-USB controller for easy data transfer to a laptop PC for filing and further processing. Fig. 1(c) shows a picture of the designed board.

The schematic of the board is shown in Fig. 2. A sine-wave voltage signal (290 mV AC amplitude with 346 mV DC average value) is generated using an AD5932 programmable function generator that is controlled by the microcontroller through a SPI interface. This signal is then amplified with a non-inverting amplifier to achieve an AC amplitude of 1.38 V, with average DC value

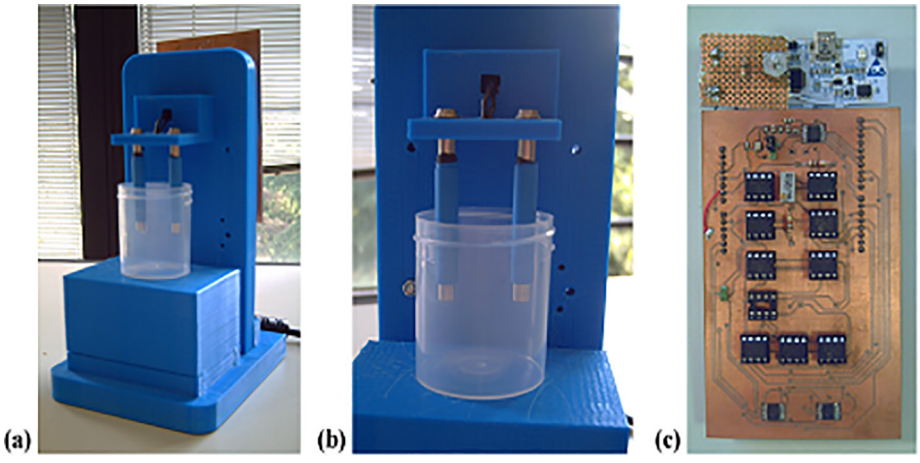

Fig. 1. Picture of the portable electronic system for Impedance Spectroscopy of liquid and semi-liquid media (a) and (b); electronic board (c).

Please cite this article in press as: M. Grossi et al., Electrical Impedance Spectroscopy (EIS) characterization of saline solutions with a low-cost portable measurement system, Eng. Sci. Tech., Int. J. (2018), https://doi.org/10.1016/j.jestch.2018.08.012

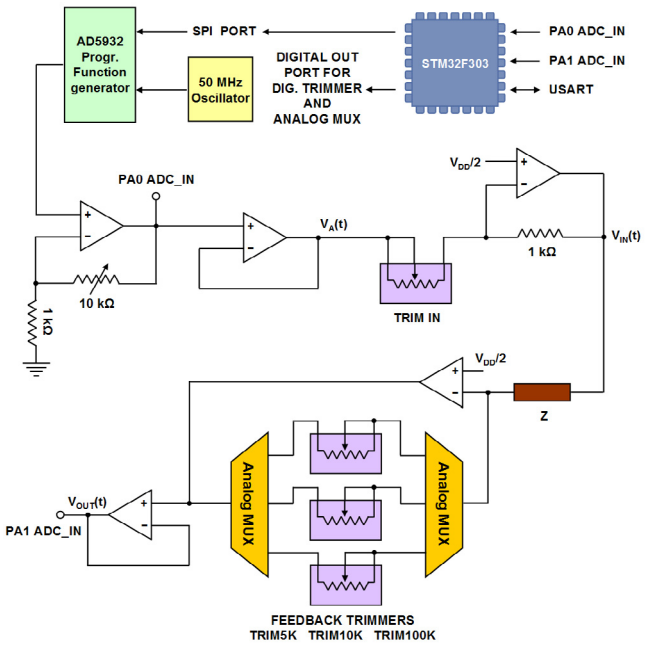

Fig. 2. Schematic of the designed electronic board.

$V_{DD}/2 = 1.65$ V. Finally, a further inverting amplifier generates the test signal $V_{in}(t)$ (i.e. a sinusoidal voltage with DC value 1.65 V and amplitude controlled by the digital potentiometer TRIM_IN), that is applied to the electrodes in direct contact with the SUT.

The current through the electrodes is then converted to a proportional voltage $V_{out}(t)$ by means of a current-to-voltage (I/V) converter, whose feedback digital potentiometers (TRIM_5K, TRIM_10K and TRIM_100K) can be selected by using two analog multiplexers to allow measurements over a wide range of impedances.

All the digital potentiometers and analog multiplexers are controlled by the microcontroller with digital signals. If

$$V_{in}(t) = \frac{V_{DD}}{2} + V_{M,in} \cdot \sin(\omega t) \quad (4)$$

the output signal

$$V_{out}(t) = \frac{V_{DD}}{2} + V_{M,out} \cdot \sin(\omega t + \varphi) \quad (5)$$

where V_{DD} is the microcontroller supply voltage (3.3 V) and the parameters $V_{M,in}$, $V_{M,out}$, φ and ω are calculated from $V_{in}(t)$ and $V_{out}(t)$ using the analog-to-digital converters (ADCs) integrated in the microcontroller and using a non-iterative algorithm based on the minimization of the mean square error [56]. The complex impedance can thus be calculated with equation (3) (where $I_{M,in}$ is determined from $V_{M,out}$ and the value of the I/V converter feedback resistance).

The system measures Re(Z) and Im(Z) spectra by testing the SUT with 37 different frequencies in the range 10 Hz–100 kHz. The test signal amplitude can be selected by the user among three different values (100 mV, 500 mV and 1 V) by setting the proper value of the digital potentiometer TRIM_IN.

A software interface, developed in LabVIEW (National Instruments), allows the user to set the measurement parameters, display the results as Bode and Nyquist plots as well as save the data on the hard disk for further analysis.

3. Results and discussion

The system discussed in Section 2 has been first tested with known impedances (realized by connecting discrete resistors and capacitors) and then using lab-prepared saline solutions.

3.1. Measurements on test impedances

A set of 14 discrete resistances (81.8, 178.3, 267, 393, 547, 811, 1200, 2680, 4630, 8205, 11875, 33200, 68750 and 120300 Ω) has been measured with the designed electronic board and the results show good accuracy compared with the values previously obtained with the LCR meter Agilent E4980A (errors <1% for frequencies <10 kHz).

Fig. 3 shows the percent error vs. frequency for a resistance value of 2680 Ω (a) and vs the resistance value for a test signal of frequency 1 kHz (b). In both cases the signal amplitude is set to 500 mV. In the case of Fig. 3(a) the full line represents the percent error in the case of a resistance value of 2680 Ω, while the dashed lines represents the minimum and maximum percent error for the full set of tested resistances: as can be seen the resistance error is below 1% for all tested resistances when f < 10 kHz, while it increases for higher frequencies up to about 3.5% for 100 kHz.

Then the following discrete impedances have been prepared and tested with the electronic board: 1) 9.9 kΩ in parallel with 1.5 nF, 2) 17.5 kΩ in parallel with 4.7 nF, 3) 54.6 kΩ in parallel with 22 nF, 4) 2.18 kΩ in series with 306 nF, 5) 21.8 kΩ in series with 306 nF, 6) 56.3 kΩ in series with 306 nF. Fig. 4 shows the Bode plots for Re(Z) and – Im(Z) in three different cases, with full lines representing measured values with the proposed system and dashed lines the expected results based on the values of resistance and capacitance measured with the commercial LCR meter.

The spectra measured for the six test impedances have been processed with the MEISP software (using the corresponding electrical circuit) to extract the value of resistance and capacitance. The results are presented in Table 1 for all test impedances and three values of signal amplitude (100 mV, 500 mV, 1 V). As can be seen, the estimated values are accurate (error lower than 1%) in most cases with higher error in the case of high impedances and small test signal (100 mV).

Overall these tests indicate that the designed board can be reliably used for EIS measurements in the frequency range 10 Hz–100 kHz on a wide range of impedances (80 Ω–120 kΩ).

3.2. Measurements on saline solutions

Four different saline solutions have been prepared: sodium chloride (NaCl) 2 M, sodium carbonate (Na_2CO_3) 2 M, potassium hydrogen phosphate (K_2HPO_4) 2 M, copper(II) sulfate ($CuSO_4$) 1 M. From each solution, different dilutions in distilled water have been created to obtain different solute molecule concentrations (hereafter simply concentration). All measurements have been carried out in triplicate at the environmental temperature T = 23.5 °C and with a voltage amplitude of 100 mV. The aim of this work is to show the feasibility of saline solution discrimination by analysis of the EIS characteristics on a wide range of frequencies and thus measurements have been carried out at constant temperature. Since the electrical conductivity of electrolytic solutions is known to increase with temperature [57], a temperature sensor has been added to the system (as discussed in Section 2). The measured temperature can thus be used to compensate the measurements for temperature variations according to some pre-calculated calibration equations.

The Bode and Nyquist plots for different concentrations of the saline solution Na_2CO_3 are presented in Fig. 5. As can be seen in Fig. 5(b), the imaginary component of the admittance Y features

Please cite this article in press as: M. Grossi et al., Electrical Impedance Spectroscopy (EIS) characterization of saline solutions with a low-cost portable measurement system, Eng. Sci. Tech., Int. J. (2018), https://doi.org/10.1016/j.jestch.2018.08.012

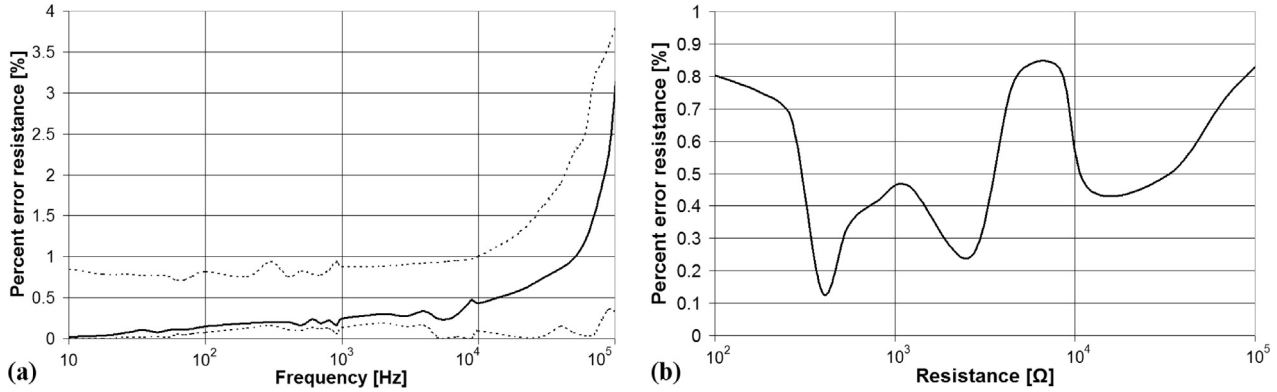

Fig. 3. Percent error on measured resistance (full line curve for a resistance value of 2680 Ω, dashed lines for the minimum and maximum values among all tested resistances) as function of frequency (a) and resistance value for frequency 1 kHz (b).

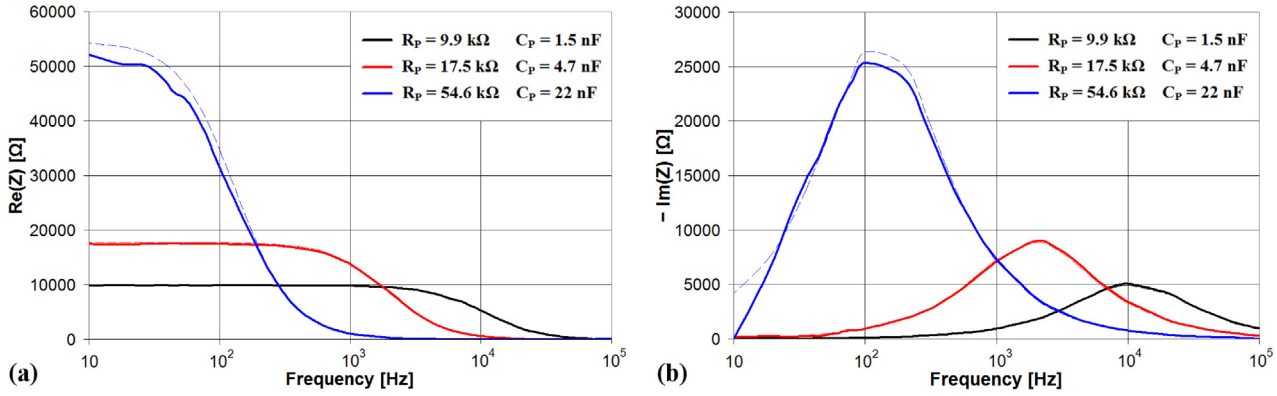

Fig. 4. Measured and theoretical values for Re(Z) and −Im(Z) in the case of impedances built from discrete resistances and capacitances.

Table 1
Estimated values of resistance and capacitance from the fitting of the measured impedance spectra.

	$V_{M,in}$ = 1 V		$V_{M,in}$ = 500 mV		$V_{M,in}$ = 100 mV	
	R (kΩ)	C (nF)	R (kΩ)	C (nF)	R (kΩ)	C (nF)
R_P = 9.9 kΩ C_P = 1.5 nF	9.94	1.56	9.91	1.57	9.88	1.92
R_P = 17.7 kΩ C_P = 4.7 nF	17.4	4.64	17.5	4.67	17.1	5.14
R_P = 54.6 kΩ C_P = 22 nF	51.3	21.7	51.9	22.4	50.1	24.7
R_S = 2.18 kΩ C_S = 306 nF	2.16	309	2.17	309	2.16	314
R_S = 21.8 kΩ C_S = 306 nF	21.7	308	21.7	309	21.5	307
R_S = 56.3 kΩ C_S = 306 nF	56.3	309	55.9	309	55.9	289

a typical inductive behavior (Im(Y) < 0) at high frequencies (>10 kHz): this is possibly caused by parasitic effects due to mutual inductance of wires and metal parts (electrodes). A proposed solution to decrease this effect is to use a 4-electrodes measurement set-up [58]. However, this allow the measurement of only the solution conductance and not the interfacial capacitance, thus preventing the correct classification of saline solutions as discussed later. Therefore, the corresponding high frequency (>10 kHz) data are discarded in the following analysis.

In the frequency range 10 Hz–10 kHz the Nyquist plot (Fig. 5(c)) is represented by a semi-circle with its center below the x-axis, and this behavior can be modeled with an equivalent electrical circuit composed of an electrical conductance G_m in series with a constant phase element (CPE) used to model a non-ideal capacitive interface. The resulting impedance is then:

$$Z = \frac{1}{G_m} + \frac{1}{Q(j\omega)^{\alpha}} = \frac{1}{G_m} + \frac{\cos\left(\frac{\alpha\pi}{2}\right)}{Q\omega^{\alpha}} - j\frac{\sin\left(\frac{\alpha\pi}{2}\right)}{Q\omega^{\alpha}} \quad (6)$$

where Q is the capacitance of the CPE and α is a parameter accounting for the non-ideality of Q (if α = 1 the CPE becomes an ideal capacitance).

The real and imaginary components of Y can be modeled as:

$$Re(Y) = \frac{Re(Z)}{|Z|^2} = \frac{\frac{1}{G_m} + \frac{\cos\left(\frac{\alpha\pi}{2}\right)}{Q\omega^{\alpha}}}{\left(\frac{1}{G_m}\right)^2 + \left(\frac{1}{Q\omega^{\alpha}}\right)^2 + \frac{2\cos\left(\frac{\alpha\pi}{2}\right)}{G_m Q\omega^{\alpha}}} \quad (7)$$

$$Im(Y) = -\frac{Im(Z)}{|Z|^2} = \frac{\frac{\sin\left(\frac{\alpha\pi}{2}\right)}{Q\omega^{\alpha}}}{\left(\frac{1}{G_m}\right)^2 + \left(\frac{1}{Q\omega^{\alpha}}\right)^2 + \frac{2\cos\left(\frac{\alpha\pi}{2}\right)}{G_m Q\omega^{\alpha}}} \quad (8)$$

The measured spectra have been fitted with the proposed model and the results are presented in Table 2 for all the saline solutions and their concentrations. The presented data show that G_m is the parameter featuring the best correlation with the solution concentration.

Fig. 6(a) shows G_m vs. solution concentration for all tested saline solutions. A very good linear correlation exists between the two variables ($R^2 > 0.99$). Two different groups can be identified, since for the same concentration Na_2CO_3 and K_2HPO_4 exhibit G_m values higher than NaCl and $CuSO_4$. This can be ascribed to the different ion concentration of the tested solutions: in fact, for the same molar concentration, Na_2CO_3 and K_2HPO_4 are characterized by double ion concentration with respect to NaCl and $CuSO_4$.

The electrical conductance, that can also be estimated with Re (Y) at high frequency (10 KHz), is not sufficient to discriminate the different types of saline solutions but can be used to estimate

Please cite this article in press as: M. Grossi et al., Electrical Impedance Spectroscopy (EIS) characterization of saline solutions with a low-cost portable measurement system, Eng. Sci. Tech., Int. J. (2018), https://doi.org/10.1016/j.jestch.2018.08.012

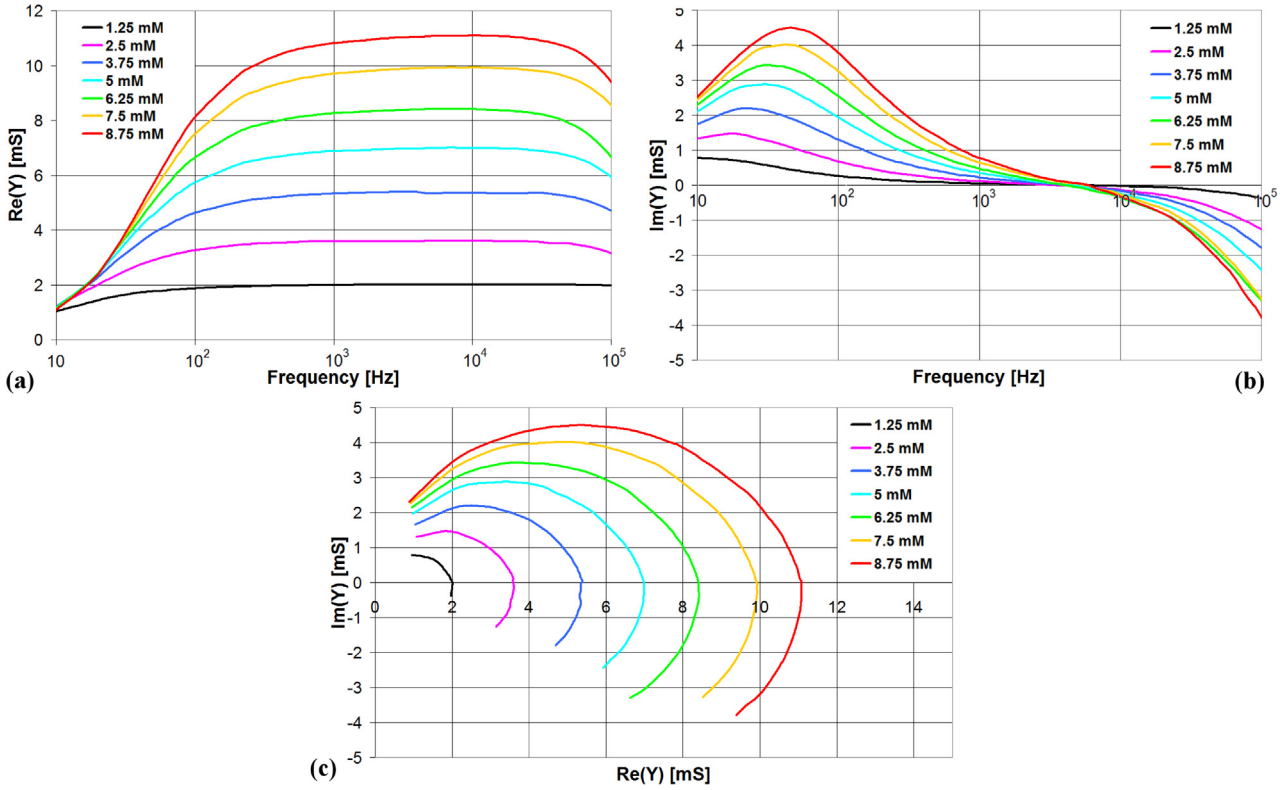

Fig. 5. Bode plots (a) and (b) and Nyquist plot (c) in the case of saline solutions of Na_2CO_3 of different molar concentrations.

Table 2
Electrical parameters of the tested saline solutions determined by fitting the measured impedance spectra with the proposed model.

Concentration (mM)	NaCl			Na_2CO_3			K_2HPO_4			$CuSO_4$		
	G_m (mS)	Q (μF)	α	G_m (mS)	Q (μF)	α	G_m (mS)	Q (μF)	α	G_m (mS)	Q (μF)	α
1.25	1.81	47.4	0.689	2.01	62.8	0.836	1.60	64.5	0.742	1.57	40.7	0.715
2.5	2.77	49.6	0.701	3.61	68.3	0.849	3.20	63.9	0.776	2.89	36.3	0.735
3.75	3.74	51.5	0.709	5.37	70.1	0.859	5.21	65.4	0.788	3.99	34.5	0.745
5	4.55	52.6	0.713	6.94	69.1	0.875	6.69	64.6	0.802	5.05	34.8	0.748
6.25	5.46	53.8	0.717	8.35	72.1	0.874	8.07	64.9	0.810	5.96	33.9	0.755
7.5	6.28	55.8	0.721	9.85	73.4	0.875	9.66	65.4	0.814	6.86	34.8	0.755
8.75	7.14	55.6	0.724	11.0	74.8	0.876	10.9	65.6	0.819	7.85	35.4	0.756

the solution concentration if the particular saline solution is known. Repeatability tests carried out in triplicate on each sample have shown that the G_m dispersion (maximum deviation among the three measurements) is always <40 μS.

The discrimination of the different saline solutions is however possible by analyzing the impedance spectrum on the full frequency range. As can be seen in Fig. 5(b) the imaginary component of Y ($Im(Y)_{max}$) features a local maximum at a frequency f_{max}. Then,

$$f_{max} = \frac{1}{2\pi} e^{\frac{1}{\alpha}\ln\left(\frac{G_m}{Q}\right)} \tag{9}$$

$$Im(Y)_{max} = \frac{G_m}{2} \cdot \frac{\sin\left(\frac{\alpha\pi}{2}\right)}{1+\cos\left(\frac{\alpha\pi}{2}\right)} \tag{10}$$

Eqs. (9) and (10) have been used to calculate f_{max} and $Im(Y)_{max}$ for all tested samples using the equivalent electrical model parameters (G_m, Q, α) estimated from the measured EIS spectrum.

Fig. 6(b) shows a scatter plot of $Im(Y)_{max}$ vs f_{max} for all tested saline solutions and concentrations. As can be seen, the couple of parameters f_{max} and $Im(Y)_{max}$ represent an electrical fingerprint allowing to discriminate the different solutions.

The scatter plot of Fig. 6 (b) has been divided in different regions corresponding to the different saline solutions. For each type of solution the linear regression line expressing $Im(Y)_{max}$ as function of f_{max} has been calculated. Then the scatter plot has been divided in four different regions so that the distance of the regression line of each type of solution from the corrsponding region edge is maximized (in the sense in mean square). The results of the application of such clustering approach is the following: if $Im(Y)_{max} > 0.065 f_{max}$ the solution is classified as Na_2CO_3; else if $Im(Y)_{max} > 0.03 f_{max}$ is K_2HPO_4; else if $Im(Y)_{max} > 0.0155 f_{max}$ it is NaCl; else it is $CuSO_4$.

Using this classification algorithm, all samples are correctly classified except for the lowest concentration (1.25 mM) of $CuSO_4$ that is misclassified as NaCl.

Once the solution type is determined, the solution concentration can be estimated from the measured value of G_m by using the calibration equations in the inset of Fig. 6(a).

Estimated solution concentrations are plotted vs the real ones in Fig. 6(c) and the high determination coefficient ($R^2 = 0.9965$)

Please cite this article in press as: M. Grossi et al., Electrical Impedance Spectroscopy (EIS) characterization of saline solutions with a low-cost portable measurement system, Eng. Sci. Tech., Int. J. (2018), https://doi.org/10.1016/j.jestch.2018.08.012

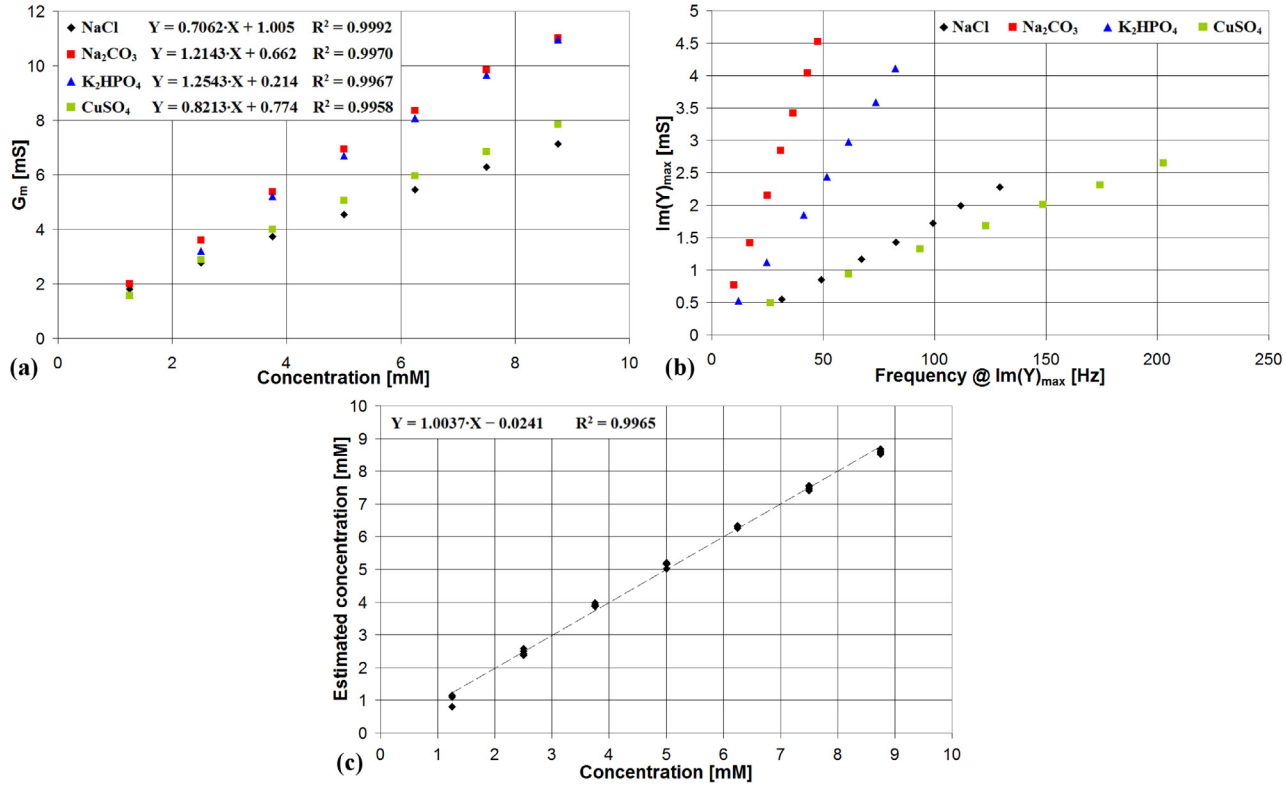

Fig. 6. Measured electrical conductance vs molar concentration for different saline solutions (a); scatter plot of peak value of Im(Y) plotted vs frequency of maximum value for different saline solutions (b); scatter plot of estimated molar concentration vs real molar concentration (c).

clearly indicates the good accuracy of the method of this work, independently of the type of saline solution.

4. Conclusions

A new low-cost portable electronic system for Electrical Impedance Spectroscopy (EIS) of liquid and semi-liquid media has been presented. The proposed system is composed of a polylactic acid structure realized with a 3D printer and an ad-hoc designed electronic board for electrical measurements, as well as for data transfer to a laptop PC by USB port for data filing and further processing.

The system has been tested with four different saline solutions (NaCl, Na_2CO_3, K_2HPO_4 and $CuSO_4$) and the results have shown that EIS spectrum provides an electrical fingerprint of the sample under test capable to discriminate the different types of solutions and to estimate their concentration with very good accuracy.

Appendix A. Supplementary data

Supplementary data associated with this article can be found, in the online version, at https://doi.org/10.1016/j.jestch.2018.08.012.

References

[1] M. Grossi, B. Riccò, Electrical impedance spectroscopy (EIS) for biological analysis and food characterization: a review, J. Sens. Sens. Syst. 6 (2017) 303–325.
[2] M. Grossi, A. Pompei, M. Lanzoni, R. Lazzarini, D. Matteuzzi, B. Riccò, Total bacterial count in soft-frozen dairy products by impedance biosensor system, IEEE Sens. J. 9 (10) (2009) 1270–1276.
[3] M. Grossi, M. Lanzoni, A. Pompei, R. Lazzarini, D. Matteuzzi, B. Riccò, An embedded portable biosensor system for bacterial concentration detection, Biosens. Bioelectron. 26 (2010) 983–990.
[4] N. Ramirez, A. Regueiro, O. Arias, R. Contreras, Electrochemical impedance spectroscopy: an effective tool for a fast microbiological diagnosis, Biotecnologia Aplicada 26 (1) (2008) 72–78.
[5] K. Settu, C.J. Chen, J.T. Liu, C.L. Chen, J.Z. Tsai, Impedimetric method for measuring ultra-low E. coli concentrations in human urine, Biosens. Bioelectron. 66 (2015) 244–250.
[6] M. Grossi, M. Lanzoni, A. Pompei, R. Lazzarini, D. Matteuzzi, B. Riccò, A portable biosensor system for bacterial concentration measurements in cow's raw milk, in: Proceedings of the 4th IEEE International Workshop on Advances in Sensors and Interfaces, (2011), 132–136.
[7] M. Grossi, R. Lazzarini, M. Lanzoni, A. Pompei, D. Matteuzzi, B. Riccò, A portable sensor with disposable electrodes for water bacterial quality assessment, IEEE Sens. J. 13 (5) (2013) 1775–1781.
[8] M. Grossi, C. Parolin, B. Vitali, B. Riccò, Bacterial concentration detection using a portable embedded sensor system for environmental monitoring, in: Proceedings of the 7th IEEE International Workshop on Advances in Sensors and Interfaces (IWASI), Vieste (FG), Italy, June 15-16 (2017), 246–251.
[9] M.Y. Jaffrin, H. Morel, Body fluid volumes measurements by impedance: a review of bioimpedance spectroscopy (BIS) and bioimpedance analysis (BIA) methods, Med. Eng. Phys. 30 (2008) 1257–1269.
[10] U.G. Kyle, I. Bosaeus, A.D. De Lorenzo, P. Deurenberg, M. Elia, J.M. Gomez, B.L. Heitmann, L. Kent-Smith, J.C. Melchior, M. Pirlich, H. Scharfetter, A. Schols, C. Pichard, Bioelectrical impedance analysis – part 1: review of principles and methods, Clin. Nutr. 23 (2004) 1226–1243.
[11] M.S. Mialich, J.M. Faccioli Sicchieri, A.J.J. Alceu, Analysis of body composition: a critical review of the use of bioelectrical impedance analysis, Int. J. Clin. Nutr. 2 (1) (2014) 1–10.
[12] R. Buendia, F. Seoane, R. Gil-Pita, Experimental validation of a method for removing the capacitive leakage artifact from electrical bioimpedance spectroscopy measurements, Meas. Sci. Technol. 21 (11) (2010) 1–8.
[13] M. Grossi, M. Lanzoni, R. Lazzarini, B. Riccò, Automatic ice-cream characterization by impedance measurements for optimal machine setting, Measurement 45 (2012) 1747–1754.
[14] M. Grossi, R. Lazzarini, M. Lanzoni, B. Riccò, A novel technique to control ice-cream freezing by electrical characteristics analysis, J. Food Eng. 106 (2011) 347–354.
[15] A. Chowdhury, T. Kanti Bera, D. Ghoshal, B. Chakraborty, Electrical impedance variations in banana ripening: an analytical study with electrical impedance spectroscopy, J. Food Process. Eng. 40 (2) (2017) 1–14.
[16] S.O. Nelson, W.C. Guo, S. Trabelsi, S.J. Kays, Dielectric spectroscopy of watermelons for quality sensing, Meas. Sci. Technol. 18 (7) (2007) 1887–1892.
[17] M. Grossi, G. Di Lecce, T. Gallina Toschi, B. Riccò, A novel electrochemical method for olive oil acidity determination, Microelectron. J. 45 (2014) 1701–1707.
[18] M. Grossi, G. Di Lecce, T. Gallina Toschi, B. Riccò, Fast and accurate determination of olive oil acidity by electrochemical impedance spectroscopy, IEEE Sens. J. 14 (9) (2014) 2947–2954.

Please cite this article in press as: M. Grossi et al., Electrical Impedance Spectroscopy (EIS) characterization of saline solutions with a low-cost portable measurement system, Eng. Sci. Tech., Int. J. (2018), https://doi.org/10.1016/j.jestch.2018.08.012

[19] M.H. Hussin, A.A. Rahim, M. Nasir, M. Ibrahim, N. Brosse, The capability of ultrafiltrated alkaline and organosolv oil palm (Elais guineensis) fronds lignin as green corrosion inhibitor for mild steel in 0.5 M HCl solution, Measurement 78 (2016) 90–103.
[20] P. Singh, M.A. Quraishi, Corrosion inhibition of mild steel using Novel Bis Schiff0s Bases as corrosion inhibitors: electrochemical and surface measurement, Measurement 86 (2016) 114–124.
[21] K.R. Ansari, M.A. Quraishi, A. Singh, Pyridine derivatives as corrosion inhibitors for N80 steel in 15% HCl: electrochemical, surface and quantum chemical studies, Measurement 76 (2015) 136–147.
[22] D. Loveday, P. Peterson, B. Rodgers, Evaluation of organic coatings with electrochemical impedance spectroscopy – part 2: application of EIS to coatings, JCT CoatingsTech (2004) 88–93.
[23] M. Mahdavian, M.M. Attar, Another approach in analysis of paint coatings with EIS measurement: phase angle at high frequencies, Corros. Sci. 48 (2006) 4152–4157.
[24] J.M. McIntyre, H.Q. Pham, Electrochemical impedance spectroscopy; a tool for organic coatings optimizations, Prog. Org. Coat. 27 (1996) 201–207.
[25] D. Andre, M. Meiler, K. Steiner, H. Walz, T. Soczka-Guth, D.U. Sauer, Characterization of high-power lithium-ion batteries by electrochemical impedance spectroscopy. II: Modelling, J. Power Sources 196 (2011) 5349–5356.
[26] R. Barton, P. Mitchell, Estimation of the residual capacity of maintenance-free lead acid batteries. Part 1. Identification of a parameter for the prediction of state-of-charge, J. Power Sources 27 (4) (1989) 287–295.
[27] J.P. Diard, B. Le Gorrec, C. Montella, EIS study of electrochemical battery discharge on constant load, J. Power Sources 70 (1998) 78–84.
[28] Z. He, F. Mansfeld, Exploring the use of electrochemical impedance spectroscopy (EIS) in microbial fuel cell studies, Energy Environ. Sci. 2 (2009) 215–219.
[29] M. Grossi, B. Riccò, An automatic titration system for oil concentration measurement in metalworking fluids, Measurement 97 (2017) 8–14.
[30] Y.H. Tang, H.C. Lin, C.L. Lai, P.Y. Chen, C.H. Lai, Mannosyl electrochemical impedance cytosensor for label-free MDA-MB-231 cancer cell detection, Biosens. Bioelectron. 116 (2018) 100–107.
[31] F. Zhang, T. Jin, Q. Hu, P. He, Distinguishing skin cancer cells and normal cells using electrical impedance spectroscopy, J. Electroanal. Chem. (2018).
[32] H.W. Kim, Y. Park, J. Yun, J. Lim, J.Z. Lee, D.G. Shin, J.H. Lee, Differentiation between normal and cancerous human urothelial cell lines using micro-electrical impedance spectroscopy at multiple frequencies, J. Med. Biol. Eng. (2018) 1–10.
[33] J. Yun, H.W. Kim, Y. Park, J.J. Cha, J.Z. Lee, D.G. Shin, J.H. Lee, Micro electrical impedance spectroscopy on a needle for ex vivo discrimination between human normal and cancer renal tissues, Biomicrofluidics 10 (3) (2016) 034109.
[34] Y. Park, H.W. Kim, J. Yun, S. Seo, C.J. Park, J.Z. Lee, J.H. Lee, Microelectrical impedance spectroscopy for the differentiation between normal and cancerous human urothelial cell lines: real-time electrical impedance measurement at an optimal frequency, Biomed. Res. Int. (2016).
[35] W. Nernst, Methode zur Bestimmung von Dielektrizitatskonstanten, Zeitschrijtfur Elektrochemie 14 (1894) 622–663.
[36] M.E. Orazem, B. Tribollet, Electrochemical Impedance Spectroscopy, John Wiley and Sons, 2008.
[37] T.K. Bera, N. Jampana, G. Lubineau, A LabVIEW-based electrical bioimpedance spectroscopic data interpreter (LEBISDI) for biological tissue impedance analysis and equivalent circuit modelling, J. Electr. Bioimpedance 7 (2016) 35–54.
[38] S. Skale, V. Doleček, M. Slemnik, Substitution of the constant phase element by Warburg impedance for protective coatings, Corros. Sci. 49 (3) (2007) 1045–1055.
[39] G. Durante, W. Becari, F.A.S. Lima, H.E.M. Peres, Electrical impedance sensor for real-time detection of bovine milk adulteration, IEEE Sens. J. 16 (4) (2016) 861–865.
[40] F.J. Ferrero, M. Valledor, J.C. Campo, Screening method for early detection of mastitis in cows, Measurement 47 (2014) 855–860.
[41] A. Chowdhury, S. Datta, T.K. Bera, D. Ghoshal, B. Chakraborty, Design and development of microcontroller based instrumentation for studying complex bioelectrical impedance of fruits using electrical impedance spectroscopy, J. Food Process Eng. 41 (1) (2018).
[42] M.A. Perez, R. Muniz, C. de la Torre, B. Garcia, C.E. Carleos, R. Crespo, L.M. Carcel, Impedance spectrometry for monitoring alcoholic fermentation kinetics under wine-making industrial conditions, XIX IMEKO World Congress Fundamental and Applied Metrology, September 6-11 2009, 2574–2578.
[43] A. Nakonieczna, B. Paszkowski, A. Wilczek, A. Szyplowska, W. Skierucha, Electrical impedance measurements for detecting artificial chemical additives in liquid food products, Food Control 66 (2016) 116–129.
[44] C.A. Olivati, A. Riul Jr., D.T. Balogh, O.N. Oliveira Jr., M. Ferreira, Detection of phenolic compounds using impedance spectroscopy measurements, Bioprocess Biosyst. Eng. 32 (2009) 41–46.
[45] N. Perini, A.R. Prado, C.M.S. Sad, E.V.R. Castro, M.B.J.G. Freitas, Electrochemical impedance spectroscopy for in situ petroleum analysis and water-in-oil emulsion characterization, Fuel 91 (2012) 224–228.
[46] E. Angelini, A. Carullo, S. Corbellini, F. Ferraris, V. Gallone, S. Grassini, M. Parvis, A. Vallan, Handheld-impedance-measurement system with seven-decade capability and potentiostatic function, IEEE Trans. Instrum. Meas. 55 (2) (2006) 436–441.
[47] AD5933 Impedance Analyzer on a chip: http://www.analog.com/media/en/technical-documentation/data-sheets/AD5933.pdf.
[48] J. Ferreira, F. Seoane, A. Ansede, R. Bragos, AD5933-based spectrometer for electrical bioimpedance applications, J. Phys. Conf. Ser. 224 (1) (2010) 012011.
[49] M. Simic, Realization of complex impedance measurement system based on the integrated circuit AD5933, Telecommunications Forum (TELFOR) (2013) 573–576.
[50] J. Hoja, G. Lentka, Portable analyzer for impedance spectroscopy, XIX IMEKO World Congress Fundamental and Applied Metrology, (2009), 497–502.
[51] L. Breniuc, V. David, C.G. Haba, Wearable impedance analyzer based on AD5933, in: International Conference and Exposition on Electrical and Power Engineering (EPE), (2014), 585–590.
[52] J. Jiang, X. Wang, R. Chao, Y. Ren, C. Hu, Z. Xu, G.L. Liu, Smartphone based portable bacteria pre-concentrating microfluidic sensor and impedance sensing system, Sens. Actuators, B 193 (2014) 653–659.
[53] D. Zhang, J. Jiang, J. Chen, Q. Zhang, Y. Lu, Y. Yao, S. Li, G. Logan Liu, Q. Liu, Smartphone-based portable biosensing system using impedance measurement with printed electrodes for 2, 4, 6-trinitrotoluene (TNT) detection, Biosens. Bioelectron. 70 (2015) 81–88.
[54] S. Sbrignadello, A. Tura, P. Ravazzani, Electroimpedance spectroscopy for the measurement of the dielectric properties of sodium chloride solutions at different glucose concentrations, J. Spectro. (2013).
[55] KiCad cross platform open source electronics design automation suite, http://kicad-pcb.org/.
[56] M. Grossi, M. Lanzoni, R. Ravazzani, B. Riccò, Linear non iterative sinusoidal fitting algorithm for microbial impedance biosensor, Sens. Transducers J. 137 (2) (2012) 235–244.
[57] R. Sauerheber, B. Heinz, Temperature effects on conductivity of seawater and physiologic saline, Chem. Sci. J. 6 (4) (2015) 1.
[58] G. Fafilek, M.W. Breiter, Instrumentation for ac four-probe measurements of large impedances, J. Electroanal. Chem. 430 (1–2) (1997) 269–278.

Please cite this article in press as: M. Grossi et al., Electrical Impedance Spectroscopy (EIS) characterization of saline solutions with a low-cost portable measurement system, Eng. Sci. Tech., Int. J. (2018), https://doi.org/10.1016/j.jestch.2018.08.012